

α_s AT LOW Q^2 FROM e^+e^- AND τ DATA*

S. Menke, Stanford Linear Accelerator Center, 2575 Sand Hill Road, Menlo Park, CA 94205, USA

Abstract

It has been shown in recent analyses by ALEPH [1] and OPAL [2] that precision QCD tests are possible with hadronic τ decays by comparing spectral moments of the hadronic decay ratio of the τ with QCD calculations. In principle e^+e^- data can be used in a similar manner by evaluating spectral moments of R . The current e^+e^- data is compared with the OPAL τ data and a prediction is made on the achievable accuracy of QCD tests with the projected precision of PEP-N [3].

1 INTRODUCTION

The τ lepton is the only lepton heavy enough to decay into hadrons. The observed spectra of the non-strange hadrons in s , where \sqrt{s} is the mass of the final state hadronic system, give the non-strange spectral functions. Decays with an even number of pions in the final state belong to the vector current while decays with an odd number of pions belong to the axial-vector current. A comparison of weighted integrals over the spectral functions of the vector and axial-vector current with QCD predictions can give fundamental parameters of the theory [4–8], including the strong coupling constant α_s . Different integrals (moments) are used to measure power corrections of non-perturbative origin and the strong coupling simultaneously, thus reducing the theoretical uncertainties on α_s connected with the non-perturbative terms.

The QCD tests can also be performed for energy scales smaller than m_τ , if the integrals over the spectral functions are performed with an upper integration limit m_τ^2 , $= s_0 \leq m_\tau^2$ and replacing m_τ^2 by m_τ^2 in the integrals [1] thus creating the spectral moments of a hypothetical τ' lepton with a mass below m_τ .

In the same manner e^+e^- annihilation into hadrons can be used to extract the spectral function of the vector-current and compare with theory by means of its spectral moments.

2 THEORY

2.1 Hadronic τ decays

The vector $v(s)$ and axial-vector $a(s)$ spectral functions (the absorptive parts of the vacuum polarization correlators) are given by the spectra in s of the final state hadrons, normalized to the branching ratios B and corrected for the phase-space:

$$v/a(s) = \frac{1}{2\pi} \text{Im}\Pi_{V/A}(s)$$

* Work supported by Department of Energy contract DE-AC03-76SF00515.

$$= \frac{m_\tau^2 \sum_{h_{V/A}} \frac{B_{\tau \rightarrow h_{V/A} \nu_\tau} w_{V/A}}{B_{\tau \rightarrow e \nu_e \nu_\tau}} \frac{N_{V/A}}{N_{V/A}} \frac{dN_{V/A}}{ds}}{6S_{\text{EW}} |V_{\text{ud}}|^2 \left(1 - \frac{s}{m_\tau^2}\right)^2 \left(1 + 2 \frac{s}{m_\tau^2}\right)}, \quad (1)$$

where the sum is performed over non-strange hadronic final states $h_{V/A}$ with angular momentum $J = 1$. $N_{V/A}$ is the number of taus that decay into the hadron $h_{V/A}$ plus neutrino, $w_{V/A}$ denotes the appropriate weight of the hadronic mode to the vector or axial-vector current, $S_{\text{EW}} = 1.0194$ is an electroweak correction term [9] and $|V_{\text{ud}}|^2 = 0.9477 \pm 0.0016$ is the squared CKM weak mixing matrix element [10].

Within the framework of QCD weighted integrals over the spectral functions (so called moments) have been calculated [11]:

$$R_{\tau,V/A}^{kl} = 6S_{\text{EW}} |V_{\text{ud}}|^2 \int_0^{m_\tau^2} \frac{ds}{m_\tau^2} \left(1 - \frac{s}{m_\tau^2}\right)^{2+k} \left(\frac{s}{m_\tau^2}\right)^l \times \left[\left(1 + 2 \frac{s}{m_\tau^2}\right) v/a(s) + v^0/a^0(s) \right], \quad (2)$$

where the scalar spectral function $v^0(s)$ vanishes, since no scalar particle has been observed in τ decays, while the pseudo-scalar spectral function $a^0(s)$ is given by the pion pole, assuming that the pion is the only pseudo-scalar final-state in non-strange τ decays:

$$a^0(s) = \frac{m_\tau^2 \frac{B_{\tau \rightarrow \pi \nu_\tau}}{B_{\tau \rightarrow e \nu_e \nu_\tau}} \delta(s - m_\pi^2)}{6S_{\text{EW}} |V_{\text{ud}}|^2 \left(1 - \frac{s}{m_\tau^2}\right)}. \quad (3)$$

The moments are used to compare the experiment with theory. In what follows, ten moments for $kl = 00, 10, 11, 12, 13$ for V and A are used. The first moments $R_{\tau,V/A}^{00}$ are the total normalized decay rates of the τ into vector and axial-vector mesons. In the naïve parton model these two rates are identical and add up to the number of colors. Since only non-strange currents are considered in this work the naïve expectation has to be multiplied by $|V_{\text{ud}}|^2$. Including the perturbative and non-perturbative contributions, equation (2) is usually written as [11]:

$$R_{\tau,V/A}^{kl} = \frac{3}{2} S_{\text{EW}} |V_{\text{ud}}|^2 \left(1 + \delta_{\text{pert}}^{kl} + \sum_{D=2,4,6,8} \delta_{V/A}^{D,kl}\right), \quad (4)$$

where $\delta_{\text{pert}}^{kl}$ are perturbative QCD corrections ($\approx 20\%$ for $kl = 00$) and the $\delta_{V/A}^{D,kl}$ terms are the so-called power corrections ($\approx 1\%$ for $kl = 00$).

The perturbative term $\delta_{\text{pert}}^{kl}$ is known to third order in α_s and partly known to fourth order in α_s . For $kl = 00$ the Contour Improved Perturbation Theory (CIPT) result is [11]:

$$\delta_{\text{pert}}^{00} = \sum_{n=1}^4 \frac{K_n}{2\pi i} \oint_{|s|=m_\tau^2} \frac{ds}{s} \left(1 - 2\frac{s}{m_\tau^2} + 2\frac{s^3}{m_\tau^6} - \frac{s^4}{m_\tau^8} \right) \left(\frac{\alpha_s(-s)}{\pi} \right)^n, \quad (5)$$

where the $K_1 = 1, K_2 = 1.63982, K_3 = 6.37101$ are known [12–16] and $K_4 = 25 \pm 50$ has been estimated [11, 17, 18]. The Taylor-expansion in $\alpha_s(m_\tau^2)$ of the CIPT result is [7, 11]:

$$\delta_{\text{pert}}^{00} = a_s + 5.2023a_s^2 + 26.366a_s^3 + (78.003 + K_4)a_s^4, \quad (6)$$

with $a_s = \alpha_s(m_\tau^2)/\pi$. It is referred to as Fixed Order Perturbation Theory (FOPT). The third method considered in this paper resums the leading term of the β -function to all orders in α_s by inserting so-called Renormalon Chains (RCPT) [19–22]. The fixed-order corrected version (up to the third order in α_s) quoted in the lower portion of table 6 in reference [20] is used in the fit.

The power corrections $\delta_{V/A}^{D,kl}$ in the framework of the Operator Product Expansion (OPE) [23] are proportional to m_τ^{-D} . The dimension $D = 2$ terms are mass-corrections of perturbative origin [7, 11] and are small for non-strange τ decays. Corrections of higher dimension are of non-perturbative origin, absorbing the long-distance dynamics into vacuum matrix elements [7, 24–26]. In contrast to the perturbative part the power corrections differ for the vector and the axial-vector currents.

If one neglects the small s -dependence of the power corrections, the $\delta_{V/A}^{D,kl}$ terms can be expressed for all kl values by a product of the power correction for $kl = 00$ and a simple integral over the kl -dependent weight-functions [11]. This approach is used for the dimension $D = 6$ and $D = 8$ terms, taking $\delta_{V/A}^{6/8,00}$ as free parameters. For the dimension $D = 2$ and $D = 4$ terms the full s -dependence is taken into account for the theoretical description of the moments [11]. The least precisely known $D = 4$ parameter, the gluon condensate which is known only to 50% [7] is also taken as a free parameter in the fit, while the $D = 2$ term is calculated from the quark masses and the strong coupling. The quark-masses and -condensates needed to complete the $D = 2, 4$ terms are taken from [7].

2.2 e^+e^- annihilation into hadrons

The ratio $R_{e^+e^-}$ is defined as:

$$\begin{aligned} R_{e^+e^-}(s) &= \frac{3s}{4\pi\alpha^2} \sigma_{e^+e^- \rightarrow \text{hadrons}}(s) \\ &= 12\pi \text{Im}\Pi^\gamma(s) = 6v^\gamma(s), \end{aligned} \quad (7)$$

with $v^\gamma(s) \approx \sum_{f=u,d,s} Q_f^2 v(s)$ being the vector spectral function with (except for the isoscalar contributions and the

charge dependent factor) similar properties as $v(s)$ in (1) and (2) and Q_f denoting the charge of the quark flavor f .

In massless perturbative QCD $\sum_f Q_f^2 v(s)$ and $v^\gamma(s)$ are identical and most conveniently expressed in form of the Adler-function [27]:

$$\begin{aligned} D_P(-s) &= -4\pi^2 s \frac{d\Pi^\gamma(-s)}{ds} \\ &= \sum_{f=u,d,s} Q_f^2 \left(1 + \sum_{n=1}^4 K_n \frac{\alpha_s^n(s)}{\pi^n} \right), \end{aligned} \quad (8)$$

with (for three flavors) the same K_n as in (5).

The mass corrections to the Adler-function are given by [28]:

$$\begin{aligned} D_{\text{mass}}(-s) &= - \sum_{f=u,d,s} Q_f^2 \frac{m_f^2(s)}{s} \left[6 + 28 \frac{\alpha_s(s)}{\pi} \right. \\ &\quad \left. + \left(259.666 - 2.25 \sum_{f'=u,d,s} \frac{m_{f'}^2(s)}{m_f^2(s)} \right) \frac{\alpha_s^2(s)}{\pi^2} \right], \end{aligned} \quad (9)$$

where the running quark masses $m_f(s)$ are calculated from scale-invariant mass parameters and an evolution equation which is known to four loops [29].

Finally the non-perturbative part of the Adler function reads [7]:

$$\begin{aligned} D_{\text{NP}}(-s) &= 8\pi^2 \sum_{f=u,d,s} Q_f^2 \left[\frac{1}{12} \left(1 - \frac{11}{18} \frac{\alpha_s(s)}{\pi} \right) \frac{\langle \frac{\alpha_s}{\pi} GG \rangle}{s^2} \right. \\ &\quad + \left(2 + \frac{2}{3} \frac{\alpha_s(s)}{\pi} \right) \frac{\langle m_f \bar{\psi}_f \psi_f \rangle}{s^2} \\ &\quad + \frac{4}{27} \frac{\alpha_s(s)}{\pi} \sum_{f'=u,d,s} \frac{\langle m_{f'} \bar{\psi}_{f'} \psi_{f'} \rangle}{s^2} \\ &\quad \left. + \frac{3}{2} \frac{\langle \mathcal{O}_6 \rangle}{s^3} + 2 \frac{\langle \mathcal{O}_8 \rangle}{s^4} \right], \end{aligned} \quad (10)$$

with the dimension 4 contributions from the gluon condensate $\langle \alpha_s/\pi GG \rangle$ and the quark condensates $\langle m_f \bar{\psi}_f \psi_f \rangle$ and the dimension 6 and 8 operators $\langle \mathcal{O}_6 \rangle$ and $\langle \mathcal{O}_8 \rangle$.

The total Adler function is simply the sum of the perturbative part (8), the mass corrections (9) and the non-perturbative part (10):

$$D(-s) = D_P(-s) + D_{\text{mass}}(-s) + D_{\text{NP}}(-s). \quad (11)$$

Moments of similar form to (2) can be defined for e^+e^- data [30]:

$$R_{e^+e^-}^{kl}(s_0) = \int_{4m_\pi^2}^{s_0} \frac{ds}{s_0} \left(1 - \frac{s}{s_0} \right)^k \left(\frac{s}{s_0} \right)^l R_{e^+e^-}(s). \quad (12)$$

In order to guarantee the validity of the OPE the endpoint in the integrals should be suppressed by at least two powers of s and the moments chosen here are therefore $kl = 20, 30, 31, 32, 33$. As in τ decays the moments can

be rewritten as integrals around the circle $|s| = s_0$ in the complex s -plane:

$$R_{e^+e^-}^{kl}(s_0) = 6\pi i \oint_{|s|=s_0} \frac{ds}{s_0} \left(1 - \frac{s}{s_0}\right)^k \left(\frac{s}{s_0}\right)^l \Pi^\gamma(s), \quad (13)$$

and further written as integrals over the Adler function after integrating by parts:

$$R_{e^+e^-}^{kl}(s_0) = \frac{3}{2\pi i} \oint_{|s|=s_0} \frac{ds}{s} \sum_{m=0}^k \frac{(-1)^m \binom{k}{m}}{m+l+1} \times \left[1 - \left(\frac{s}{s_0}\right)^{m+l+1} \right] D(s). \quad (14)$$

In the QCD fits the dimension $D = 6$ and $D = 8$ terms are fitted using $\langle \mathcal{O}_{6,8} \rangle$ as free parameters. Note that this differs from the τ data fits where the contributions to the moment $kl = 00$ are used as free parameters. For the dimension $D = 2$ and $D = 4$ terms the full s -dependence is taken into account for the theoretical description of the moments as described above. In contrast to the non-strange τ data where the least precisely known $D = 4$ parameter is the gluon condensate the largest uncertainty for the e^+e^- data comes from the strange quark mass $m_s(1 \text{ GeV})$ which is used as a free parameter for the $D = 2$ and $D = 4$ terms. The other quark-masses and -condensates needed to complete the $D = 2, 4$ terms are taken from [7].

3 RESULTS OF QCD FITS TO τ DATA

The fit results of QCD parameters to the ten moments $R_{\tau,V/A}^{kl}$ for $kl = 00, 10, 11, 12, 13$ as reported in [2, 31] are shown in Tab. 1. Only the CIPT fits are presented here, since the focus is the stability of the QCD fits and the two other approaches lead to similar results within the theoretical uncertainties. The various fits demonstrate the stability of the method and that the perturbative parameter α_s can be measured together with the non-perturbative parts even if most of the non-perturbative parts do not cancel as it is the case in the first three fits.

Note that the statistical error on α_s in the last two fits is different only because the last fit uses additional information from the τ lifetime and the leptonic branching ratios [2].

The extension to energy scales $s < m_\tau^2$ is demonstrated in Fig. 1. Here the moment $R_{\tau',V+A}^{00}(s_0 = m_{\tau'}^2)$ is shown together with the fit results to the three different theories FOPT, CIPT and RCPT for the perturbative part plus non-perturbative parts.

The error on the theoretical curves (or alternatively their spread) indicates that the OPE is applicable to values as low as 1.5 GeV^2 which can be used to extract the running of the strong coupling constant from τ data alone.

The three considered theories differ in the treatment of unknown higher order terms which is partially taken into account as theoretical uncertainty by means of the error on

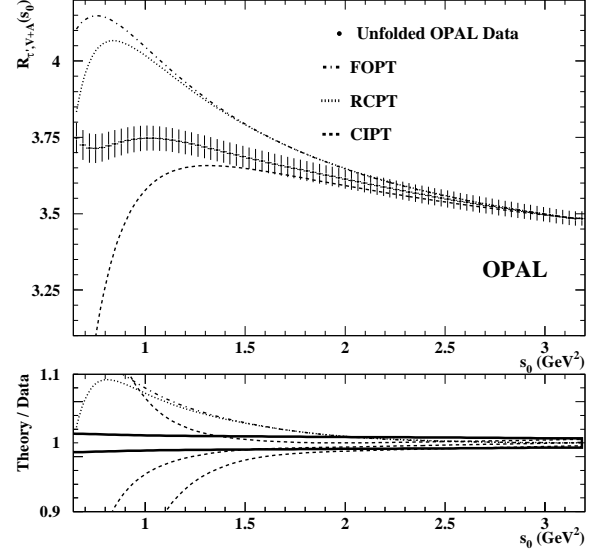


Figure 1: $R_{\tau'}^{V+A}(s_0)$ for a hypothetical τ' lepton versus the upper integration limit $s_0 = m_{\tau'}^2$.

K_4 . As a conservative approach one could take the average of all three results and their spread as additional theoretical uncertainty. From the results in [2] one obtains therefore:

$$\alpha_s(m_\tau^2) = 0.326 \pm 0.007_{\text{exp}} \pm 0.022_{\text{theo}}, \quad (15)$$

which translates to

$$\alpha_s(m_Z^2) = 0.1194 \pm 0.0008_{\text{exp}} \pm 0.0027_{\text{theo}} \quad (16)$$

at $m_Z = 91.188 \text{ GeV}$.

4 AVERAGING OF e^+e^- DATA

Exclusive e^+e^- channels up to a CMS energy of 2.2 GeV [32–60] are combined in this analysis to calculate the total hadronic cross section. The narrow ω and ϕ resonances are excluded from the exclusive channels and added to the total cross section as relativistic Breit-Wigner curves with s -dependent widths [10, 61]. The weights of individual channels and the treatment of systematic errors is taken from [30] but the statistical errors and the final result are obtained in a slightly different manner:

1. a common equidistant binning in energy is chosen for all channels ($N = 300$ bins from $E_{\text{min}} = 0 \text{ GeV}$ to $E_{\text{max}} = \sqrt{5} \text{ GeV}$) and for every experiment and channel a histogram is filled with weighted averages of cross section measurements falling in the same bin:

$$d_i = \frac{\sum_{\{j|NE_j/E_{\text{max}} \in [i-1, i]\}} \sigma_j / \Delta^2 \sigma_j}{\sum_{\{j|NE_j/E_{\text{max}} \in [i-1, i]\}} 1 / \Delta^2 \sigma_j}, \quad i = 1 \dots N, \quad (17)$$

Table 1: Comparison of the QCD fit results (CIPT) to the moments of vector (axial-vector) current, the simultaneous fit of all moments for both currents, and the moments for the sum of both currents [31]. The quoted errors contain statistical errors only.

observable	V		A		V and A		V + A	
	value	error	value	error	value	error	value	error
$\alpha_s(m_\tau^2)$	0.341	± 0.017	0.357	± 0.019	0.347	± 0.012	0.348	± 0.009
$\langle \frac{\alpha_s}{\pi} GG \rangle / \text{GeV}^4$	0.002	± 0.010	-0.011	± 0.020	0.001	± 0.008	-0.003	± 0.011
δ_V^6	0.0259	± 0.0041	—	—	0.0256	± 0.0034	—	—
δ_V^8	-0.0078	± 0.0018	—	—	-0.0080	± 0.0013	—	—
δ_A^6	—	—	-0.0246	± 0.0086	-0.0197	± 0.0033	—	—
δ_A^8	—	—	0.0067	± 0.0050	0.0041	± 0.0019	—	—
δ_{V+A}^6	—	—	—	—	—	—	0.0012	± 0.0047
δ_{V+A}^8	—	—	—	—	—	—	-0.0010	± 0.0029
$\chi^2/\text{d.o.f.}$	0.07/1		0.06/1		0.63/4		0.16/1	

where the squared errors Δ_i^2 are given by the inverse of the denominator in (17).

- gaps at $k = i \dots j$ between bins i and j of individual measurements are interpolated with the trapezoidal rule:

$$d_k = c_k d_i + (1 - c_k) d_j, \quad c_k = \frac{k - i}{j - i}. \quad (18)$$

- the statistical errors are interpolated with the same procedure:

$$\Delta_k = c_k \Delta_i + (1 - c_k) \Delta_j, \quad (19)$$

and are therefore larger compared to Gaussian propagated errors by the factor:

$$r_k = \frac{c_k \Delta_i + (1 - c_k) \Delta_j}{c_k \Delta_i \oplus (1 - c_k) \Delta_j}. \quad (20)$$

- the correlation matrix for the interpolated parts is given by:

$$V_{kl}^{\text{stat}} = r_k r_l (c_k c_l \Delta_i^2 + (1 - c_k)(1 - c_l) \Delta_j^2). \quad (21)$$

- the systematic errors are also interpolated according to the trapezoidal rule (19) and all systematic errors are assumed to be 100% correlated.
- the final error matrix is given by the sum of both:

$$V_{kl} = V_{kl}^{\text{stat}} + V_{kl}^{\text{sys}}. \quad (22)$$

- the averaged cross section over all experiments in bin i for one exclusive channel is obtained from the weighted mean of all measurements and its error by usual error propagation. In case of inconsistent sets of data points for a particular bin its final error is scaled by the ratio $S = \sqrt{\chi^2 / \chi_{68\%}^2}$, if $S > 1$, where χ^2 is the calculated χ^2 for the individual experiments being consistent with the average and $\chi_{68\%}^2$ is the χ^2 value corresponding to a confidence level of 68%.

After this interpolation and averaging procedure the total hadronic cross section is given by the sum of the exclusive channels as in [30]. The resulting values for $R_{e^+e^-}$ are shown in Fig. 2.

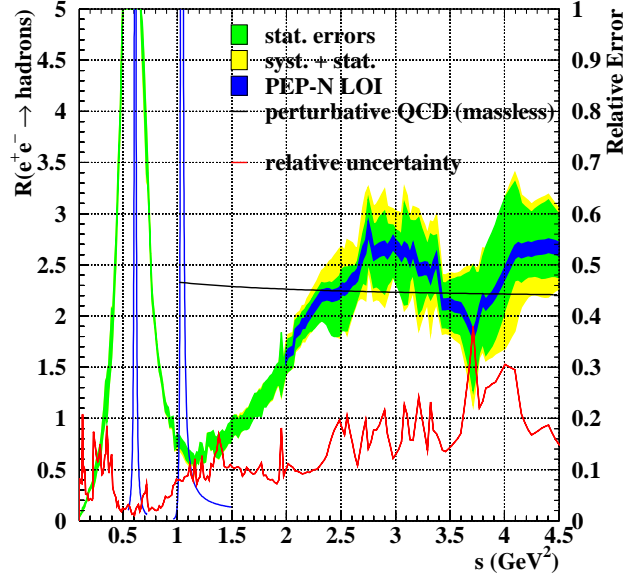


Figure 2: $R_{e^+e^-}(s)$ from exclusive channels. The dark gray band denotes statistical errors; the light gray band shows the sum of systematic and statistical errors. The dark solid line shows the relative uncertainty; the small dark error band beyond $s = 2 \text{ GeV}^2$ shows the projected uncertainty after 5 years of PEP-N [3]. The narrow ω and ϕ resonances and the massless QCD prediction are also indicated by solid lines.

5 RESULTS OF QCD FITS TO e^+e^- DATA

The five moments $R_{e^+e^-}^{kl}(4\text{ GeV}^2)$ for $kl = 20, 30, 31, 32, 33$ are given in Tab. 2. Their correlations are given in Tab. 3. The result of the CIPT fit to these moments is given in Tab. 4. The correlations of the fit parameters are shown in Tab. 5.

Table 2: Moments $R_{e^+e^-}^{kl}(4\text{ GeV}^2)$ for $kl = 20, 30, 31, 32, 33$ from exclusive e^+e^- data. The errors include statistical and systematic uncertainties; projected errors after 5 years running of PEP-N and theoretical uncertainties are also given.

kl	$R_{e^+e^-}^{kl}$	stat.+sys.	PEP-N	theo.
20	0.760	0.014	0.009	0.008
30	0.569	0.008	0.007	0.012
31	0.1206	0.0027	0.0016	0.0040
32	0.0355	0.0015	0.0006	0.0000
33	0.0143	0.0009	0.0003	0.0000

Table 3: Correlations of the moments $R_{e^+e^-}^{kl}(4\text{ GeV}^2)$ for $kl = 20, 30, 31, 32, 33$ in percent. The values correspond to the quadratic sum of experimental and theoretical errors.

kl	30	31	32	33
20	+86.6	+3.8	+74.5	+70.4
30		-44.2	+33.6	+30.0
31			+54.9	+50.9
32				+98.8

Table 4: Results from the QCD fits to the moments $R_{e^+e^-}^{kl}(4\text{ GeV}^2)$ for $kl = 20, 30, 31, 32, 33$ from exclusive e^+e^- data. The errors include statistical and systematic uncertainties; projected errors after 5 years running of PEP-N and theoretical uncertainties are also given.

obs.	val.	err.	PEP-N	theo.
$\alpha_s(4\text{ GeV}^2)$	0.286	0.031	0.027	0.015
m_s/GeV	0.220	0.036	0.026	0.059
$\langle\mathcal{O}_6\rangle/\text{GeV}^6$	-0.0041	0.0007	0.0005	0.0002
$\langle\mathcal{O}_8\rangle/\text{GeV}^8$	0.0043	0.0004	0.0002	0.0002
$\chi^2/\text{d.o.f.}$	0.04/1			

The value of the strong coupling at 4 GeV^2 corresponds to

$$\alpha_s(m_Z^2) = 0.117 \pm 0.005_{\text{exp}} \pm 0.002_{\text{theo}} \quad (23)$$

at $m_Z = 91.188\text{ GeV}$ in good agreement with the τ result 16 but with a larger experimental uncertainty. Figure 3

Table 5: Correlations of the QCD fit parameters to the moments $R_{e^+e^-}^{kl}(4\text{ GeV}^2)$ for $kl = 20, 30, 31, 32, 33$ in percent. The values correspond to the quadratic sum of experimental and theoretical errors.

obs.	m_s	$\langle\mathcal{O}_6\rangle$	$\langle\mathcal{O}_8\rangle$
α_s	+77.2	+71.4	-42.0
m_s		+35.9	-8.2
$\langle\mathcal{O}_6\rangle$			-93.2

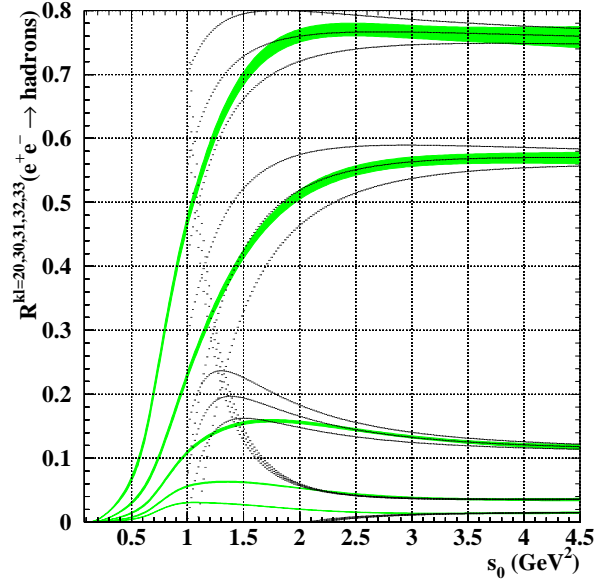


Figure 3: The moments $R_{e^+e^-}^{kl=20,30,31,32,33}(s_0)$ versus the integration limit s_0 . The shaded bands show the experimental moments with statistical and systematic uncertainties from top to bottom in the order $kl = 20, 30, 31, 32, 33$. The dotted curves denote central values and $\pm 1\sigma$ ranges for the theoretical expectations (CIPT) using the fit values to the moments at $s_0 = 4\text{ GeV}^2$ as input.

shows the moments of $R_{e^+e^-}$ as a function of the upper integration limit together with theoretical predictions using the fitted values at $s_0 = 4\text{ GeV}^2$ as input. Reasonable agreement between the extrapolated and the measured moments is observed for all five moments down to $s_0 \approx 2.5\text{ GeV}^2$. The first three moments agree within errors with the extrapolated results down to $s_0 \approx 1.5\text{ GeV}^2$.

6 CONCLUSIONS

The comparison of QCD fits to different currents (V, A, V and A, V+A) in non-strange hadronic τ decays probes the stability of the OPE at low energy scales. The good agreement of perturbative and non-perturbative parameters among these fits demonstrates that QCD fits can reliably be performed at these low energy scales. The use of spec-

tral moments is therefore extended to $e^+e^- \rightarrow$ hadrons data in order to fit QCD parameters at 4 GeV^2 . While the extraction of the strong coupling α_s is not competitive in terms of experimental uncertainties with the measurement from τ data it provides an important cross check and probes an energy region not accessible with τ decays. Furthermore the sensitivity to the mass of the strange quark can be used to constrain this parameter. A value of $m_s(1 \text{ GeV}) = (220 \pm 36 \pm 59) \text{ MeV}$ has been observed. The experimental uncertainty could be reduced by 30 % after 5 years of running with PEP-N.

7 ACKNOWLEDGMENTS

I would like to thank the organizers Stan Brodsky and Rinaldo Baldini for giving me the opportunity to present this work. I am also indebted to Andreas Höcker who provided me with FORTRAN files of the e^+e^- data.

8 REFERENCES

- [1] ALEPH Collaboration, R. Barate et al., Eur. Phys. J. **C4** (1998) 409.
- [2] OPAL Collaboration, K. Ackerstaff et al., Eur. Phys. J. **C7** (1999) 571.
- [3] R. Baldini et al., <http://www.slac.stanford.edu/grp/rd/epac/LOI/LOI-2000.3-Experiment.pdf> (2000).
- [4] E. Braaten, Phys. Rev. Lett. **60** (1988) 1606.
- [5] E. Braaten, Phys. Rev. **D39** (1989) 1458.
- [6] S. Narison and A. Pich, Phys. Lett. **B211** (1988) 183.
- [7] E. Braaten, S. Narison, and A. Pich, Nucl. Phys. **B373** (1992) 581.
- [8] F. Le Diberder and A. Pich, Phys. Lett. **B286** (1992) 147.
- [9] W.J. Marciano and A. Sirlin, Phys. Rev. Lett. **61** (1988) 1815.
- [10] D.E Groom et al., Eur. Phys. J. **C15** (2000) 1.
- [11] F. Le Diberder and A. Pich, Phys. Lett. **B289** (1992) 165.
- [12] K.G. Chetyrkin, A.L. Kataev, and F.V. Tkachev, Phys. Lett. **B85** (1979) 277.
- [13] M. Dine and J. Sapirstein, Phys. Rev. Lett. **43** (1979) 668.
- [14] W. Celmaster and R.J. Gonsalves, Phys. Rev. Lett. **44** (1980) 560.
- [15] S.G. Gorishnii, A.L. Kataev, and S.A. Larin, Phys. Lett. **B259** (1991) 144.
- [16] L.R. Surguladze and M.A. Samuel, Phys. Rev. Lett. **66** (1991) 560, Erratum: *ibid.* **66** (1991) 2416.
- [17] A. Pich, **FTUV-97-03** (1997).
- [18] A.L. Kataev and V.V. Starshenko, Mod. Phys. Lett. **A10** (1995) 235.
- [19] P. Ball, M. Beneke, and V.M. Braun, Nucl. Phys. **B452** (1995) 563.
- [20] M. Neubert, Nucl. Phys. **B463** (1996) 511.
- [21] C.N. Lovett-Turner and C.J. Maxwell, Nucl. Phys. **B452** (1995) 188.
- [22] C.J. Maxwell and D.G. Tonge, Nucl. Phys. **B481** (1996) 681.
- [23] K.G. Wilson, Phys. Rev. **179** (1969) 1499.
- [24] M.A. Shifman, A.I. Vainshtein, and V.I. Zakharov, Nucl. Phys. **B147** (1979) 385.
- [25] M.A. Shifman, A.I. Vainshtein, and V.I. Zakharov, Nucl. Phys. **B147** (1979) 448.
- [26] M.A. Shifman, A.I. Vainshtein, and V.I. Zakharov, Nucl. Phys. **B147** (1979) 519.
- [27] S.L. Adler, Phys. Rev. **D10** (1974) 3714.
- [28] K. Chetyrkin and J. Kühn, Phys. Lett. **B248** (1990) 359.
- [29] J. Vermaseren, S. Larin, and T. van Ritbergen, Phys. Lett. **B405** (1997) 327.
- [30] M. Davier and A. Höcker, Phys. Lett. **B419** (1998) 419.
- [31] S. Menke, BONN-IR-98-13.
- [32] L. M. Barkov et al., Nucl. Phys. **B256** (1985) 365.
- [33] I. B. Vasserman et al., Yad. Fiz. **30** (1979) 999.
- [34] I. B. Vasserman et al., Yad. Fiz. **33** (1981) 709.
- [35] S. R. Amendolia et al., Phys. Lett. **B138** (1984) 454.
- [36] A. Quenzer et al., Phys. Lett. **B76** (1978) 512.
- [37] DM2, D. Bisello et al., Phys. Lett. **B220** (1989) 321.
- [38] CMD-2, A. Bondar et al., talk at ICHEP 2000, Osaka, Japan (2000).
- [39] S. I. Dolinsky et al., Phys. Rept. **202** (1991) 99.
- [40] G. Cosme et al., Phys. Lett. **B63** (1976) 349.
- [41] G. Parrou et al., Phys. Lett. **B63** (1976) 357.
- [42] G. Cosme et al., Nucl. Phys. **B152** (1979) 215.
- [43] A. Cordier et al., Nucl. Phys. **B172** (1980) 13.
- [44] DM2, A. Antonelli et al., Z. Phys. **C56** (1992) 15.
- [45] M. Achasov et al., Phys. Lett. **B462** (1999) 365.
- [46] L. M. Kurdadze et al., JETP Lett. **43** (1986) 643.
- [47] DM2, D. Bisello et al., Nucl. Phys. Proc. Suppl. **21** (1991) 111.
- [48] B. Esposito et al., Lett. Nuovo Cim. **28** (1980) 195.
- [49] L. M. Barkov et al., Sov. J. Nucl. Phys. **47** (1988) 248.
- [50] A. Cordier et al., Phys. Lett. **B109** (1982) 129.
- [51] CMD-2, R. R. Akhmetshin et al., Phys. Lett. **B475** (2000) 190.
- [52] DM2, A. Antonelli et al., Phys. Lett. **B212** (1988) 133.
- [53] D. Bisello et al., Phys. Lett. **B107** (1981) 145.
- [54] P. M. Ivanov et al., Phys. Lett. **B107** (1981) 297.
- [55] P. m. Ivanov et al., JETP Lett. **36** (1982) 112.
- [56] B. Delcourt et al., Phys. Lett. **B99** (1981) 257.
- [57] F. Mane et al., Phys. Lett. **B99** (1981) 261.
- [58] DM2, D. Bisello et al., Z. Phys. **C39** (1988) 13.
- [59] A. Cordier et al., Phys. Lett. **B110** (1982) 335.
- [60] F. Mane et al., Phys. Lett. **B112** (1982) 178.
- [61] S. Eidelman and F. Jegerlehner, Z. Phys. **C67** (1995) 585.